Polarization of protons by the spin-refrigerator mechanism in yttrium ethyl sulfate

J. Sowinski* and L. D. Knutson
Department of Physics, University of Wisconsin–Madison, Madison, Wisconsin 53706
(Received 17 September 1987)

Proton polarizations in excess of 50% have been achieved in single crystals of $Y(C_2H_5SO_4)_3\cdot 9H_2O$ doped with about 0.01 at.% Yb. The protons are polarized by the spin-refrigerator process, in which the crystals are rotated in a magnetic field at low temperature. Typical operating parameters are $F = 40$–90 revolutions/sec, $H = 9$–11 kOe, and $T = 0.6$ K. Measurements of the maximum polarization and of polarization-buildup curves are presented for a variety of operating conditions. These results are found to be in reasonably good agreement with predictions obtained from model calculations which simulate the polarization mechanism at the atomic level. The calculations show that multiple–spin-flip processes are important, and that these processes produce a significant reduction in the maximum attainable proton polarization. Measurements of the proton spin-relaxation time are also reported. Relaxation times in excess of 100 h were observed for magnetic fields of less than 1 kOe.

I. INTRODUCTION

Spin-polarized proton targets are important research tools in both nuclear and high-energy physics. In order to make advances in polarized-target technology it is necessary to develop a good understanding of the underlying solid-state physics. In particular, one needs to be concerned with the interaction of electronic and nuclear spins with each other and with the lattice.

In the early 1960s two quite different methods were proposed for achieving large nuclear polarizations. One method makes use of the "solid-state effect" in which microwaves are used to drive forbidden transitions between hyperfine levels in materials containing hydrogen. By as early as 1962 Schmugge and Jeffries[1] had achieved sizable dynamic nuclear polarizations in single crystals of Nd-doped $La_2Mg_3(NO_3)_{12}\cdot 24H_2O$, and in the intervening years there have been continuing advances in the technology and understanding of these targets. To date, nearly all of the polarized proton targets used in nuclear and high-energy physics research have been based on the microwave pumping technique. In 1963 Jeffries[2] and Abragam[3] independently proposed an alternate scheme for polarizing protons. In this method the nuclear polarization is achieved by rotating a crystal containing paramagnetic ions which have a highly anisotropic g factor in a magnetic field at low temperatures. Devices which make use of this mechanism are commonly referred to as "spin refrigerators."

Early researchers[4–10] found that Yb-doped yttrium

cent set of experiments Felcher *et al.*[13] were unsuccessful in matching the results of Button-Shafer *et al.*, achieving a maximum polarization of only 41%.

A substantial amount of theoretical work on the spin-refrigerator process in YES has been done, primarily in conjunction with the early spin-refrigerator experiments.[4–10] While many of the properties of YES are now well understood, there does not yet exist a single comprehensive "theory" which has been thoroughly tested against experiment and which can be used with confidence to predict the behavior of spin-refrigerator targets under a wide range of operating conditions.

In the present paper we report on a series of measurements undertaken to further investigate the YES spin-refrigerator mechanism, with a final goal of producing a polarized proton target for use in nuclear physics experiments. In particular, we have obtained new measurements of polarization buildup curves, maximum polarizations and nuclear spin-relaxation rates. The primary difference between the present experiment and the recent work of Refs. 11–13 is that our results have been obtained at temperatures well below 1 K. In conjunction with the experimental work, we have developed a computer-based model of the polarization buildup process. This model provides theoretical predictions for comparison with the experimental results, and may also be used as a guide for optimizing the polarized target parameters.

The necessary theoretical background is presented in Sec. II. In Sec. III we describe the equipment and experi-

II. THEORETICAL BACKGROUND

A. The spin-refrigerator mechanism

The basic idea of the spin refrigerator is simple. Paramagnetic ions in a crystal at low temperature and in a high magnetic field can have a substantial polarization at thermal equilibrium. Here the ion polarization P_e is defined as

$$P_e=\frac{N(m_I=+\frac{1}{2})-N(m_I=-\frac{1}{2})}{N(m_I=+\frac{1}{2})+N(m_I=-\frac{1}{2})}\ , \qquad (1)$$

where N is the number of ions with magnetic quantum number m_I, and where we have assumed for simplicity that the ions have spin $\frac{1}{2}$. The polarization of the protons, P_n, is defined in an analogous manner in terms of the proton magnetic substate populations. In this case the substates are labeled by the quantum number m_s. If one uses a crystal in which the g factor of the ions, g_e, is highly anisotropic, or more precisely in which the g_e approaches zero for some orientation of the magnetic field, the polarization of the ions can be transferred to the protons. This is accomplished by simply rotating the crystal relative to the magnetic field. As the crystal rotates the g_e becomes small and for some orientation will be equal to the proton g factor g_p. At this point (referred to as the crossover point) mutual spin flips of a proton with an ion are energetically allowed and occur readily.

The process for transfer of the polarization is represented in Fig. 1. Here we show energy level diagrams for a system consisting of one proton and one ion (assumed again to be spin $\frac{1}{2}$). The states are labeled with the sign of the magnetic quantum numbers using the notation $|m_I m_s\rangle$. Figure 1(a) corresponds to an orientation of the crystal for which the g_e is large. Here the energy splitting between the ion magnetic substrates is large compared to kT. If the crystal is kept in this orientation for a time which is long compared to the ion spin-lattice relaxation time, ions in the states $|+,-\rangle$ and $|+,+\rangle$ decay to $|-,-\rangle$ and $|-,+\rangle$, respectively; i.e., the ions reach thermal equilibrium and become highly polarized. If the crystal is then rotated to the crossover point in a time which is short compared to the relaxation time, the polarization is maintained and one obtains an energy level diagram as shown in Fig. 1(b). At this point the states $|-,-\rangle$ and $|+,+\rangle$ mix, and the ion and proton spin temperatures equalize through energy allowed mutual spin flips. The crystal is then rotated back to the orientation of Fig. 1(a), and when thermal equilibrium is reached the net result is that ion-proton pairs in the state $|-,-\rangle$ have been transferred to the state $|-,+\rangle$. In practice, each ion in the crystal can transfer its polarization to any one of a number of neighboring protons, while protons which are far from any ion become polarized by spin diffusion. Consequently, protons throughout the sample acquire a sizable polarization after a sufficient number of spin-refrigerator cycles have elapsed. If one assumes that each spin flip involves only a single proton and a single ion and that the nuclear spin-relaxation time is long compared to the polarizing time, one expects that the proton polarization will approach the polarization of the ions at the crossover point.

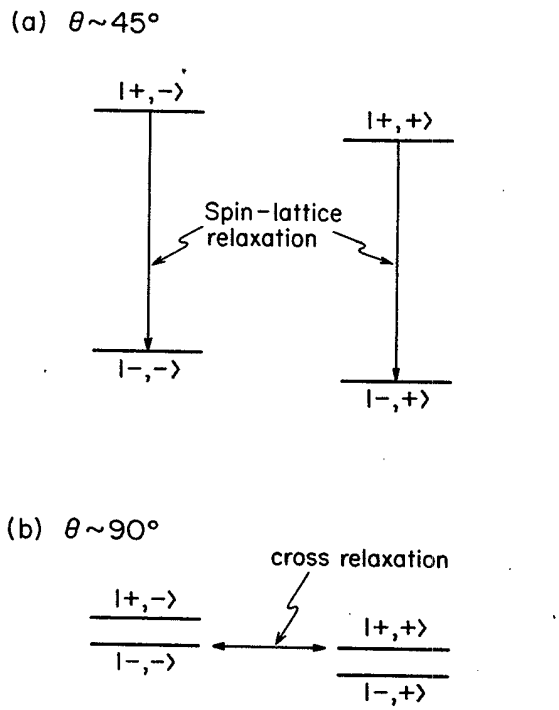

FIG. 1. Illustration of the process by which protons are polarized in a spin refrigerator. The level structure in (a) corresponds to an orientation of the crystal for which the ion g factor is large, and the spins couple strongly to the lattice ($\sim 45°$ for YES), while (b) represents the cross relaxation point ($\sim 0°$ for YES) where the ion and proton g factors are equal.

The origin of the name spin refrigerator is now apparent. The ions act as the coolant. As the crystal is rotated toward the crossover point, g_e decreases and the ion spin temperature therefore decreases. When g_e is equal to g_p, the protons and ions come into thermal contact and the spin temperatures equalize. As the crystal is rotated back to its original orientation the ion spin temperature increases once more, and the heat is exhausted to the lattice.

B. Yttrium ethyl sulfate spin refrigerator

Yttrium ethyl sulfate, $Y(C_2H_5SO_4)_3\cdot 9H_2O$, doped with ytterbium ions has many properties which make it well suited for use in a spin refrigerator. The $^2F_{7/2}$ ground state of the ytterbium ion is split by the crystal field into four doublets. At liquid He temperatures only the lowest doublet, which has $m_J=\pm\frac{1}{2}$, is populated. The purity of the $m_J=\pm\frac{1}{2}$ doublet is a direct result of the hexagonal symmetry of the YES crystal.[5]

Each doublet is further split by external magnetic fields. The ion g factor is given by

$$g_e=(g_\parallel^2\cos^2\theta+g_\perp^2\sin^2\theta)^{1/2}\ , \qquad (2)$$

where θ is the angle between the applied magnetic field and the crystal c axis. For a pure $m_J=\pm\frac{1}{2}$ doublet it is

straightforward to show that $g_\perp = 0$ and $g_\parallel = 3.43$. The measured[14] value of $g_\parallel$ is 3.328 ± 0.005. The small discrepancy with the theoretical prediction has been attributed to lattice vibrations (the effect of static crystal field mixing with the $J = \frac{5}{2}$, $m_J = \pm\frac{3}{2}$ excited states is thought to be too small to account for the discrepancy). A nonzero value of $g_\perp$ can result from crystal distortions[7] and impurities. No direct measurement of $g_\perp$ has ever been made; however, the success of YES spin refrigerators suggests that $g_\perp$ is smaller than g_p. From measurements of polarization-buildup curves for YES spin refrigerators, Potter and Stapleton[10] have concluded that $g_\perp \simeq 0.3 g_p$.

The Yb ions in YES also have a favorable spin-lattice relaxation rate, T_{1e}^{-1}. For temperatures below a few K the relaxation is dominated by the direct single phonon process[5] for which

$$T_{1e}^{-1} = AH^5 \sin^2\theta \cos^3\theta \coth\chi \ \sec^{-1} , \tag{3}$$

where A is a constant, H is the magnetic field in Oe,

$$\chi = g_\parallel H \mu_B \cos\theta / 2kT , \tag{4}$$

and μ_B is the Bohr magneton. Measurements by Wolfe and Jeffries[14] of the angular dependence of T_{1e}^{-1} agree with Eq. (3) for angles less than 45°. (The discrepancies at larger angles are attributed to a phonon bottleneck, which should be unimportant in our work, since our Yb concentrations are typically 2 orders of magnitude lower than those of Ref. 14.) From their measurements, Wolfe and Jeffries[14] extract the result $A = 2.40 \times 10^{-17}$, which is in reasonably good agreement with the theoretical value. Note that the relaxation rate is largest for $\theta \sim 45°$ and goes to zero at $\theta = 90°$. Since the ions couple strongly to the lattice when g_e is moderately large, one can obtain large ion polarizations. Moreover, the polarization is maintained as the crystal is rotated to the crossover point at $\theta = 90°$. Because of the favorable angular dependence of T_{1e}^{-1}, it is possible to obtain sizable proton polarizations by simply rotating the crystal at a constant rate.

From Eqs. (2) and (3) one can easily predict the ion polarization at crossover (denoted by P_{es}) for a given temperature, magnetic field and rotation rate. Figure 2 shows calculations of this quantity for $H = 11$ kOe and for temperatures of 1.2 K and 0.62 K, typical of pumped ^{4}He and pumped ^{3}He systems, respectively. Note that at the lower temperature one can obtain large ion polarizations at crossover for much lower rotation rates. Since our polarized target requirements involve the use of very large samples, the lower rotation rates are highly desirable, and for this reason we decided to build a system that operates near 0.6 K.

In order to obtain large proton polarizations it is necessary that the proton spin-relaxation time, T_{1n}, be long compared to the time required to polarize the target. Previous experimenters,[5,8] working in the 1–2 K range, have found that the holding times meet this criterion and are well described by a process in which proton spin flips occur through a dipole-dipole interaction with the Yb ions as the Yb spins relax to the lattice. The nuclear spin-relaxation rate for this process, first calculated by

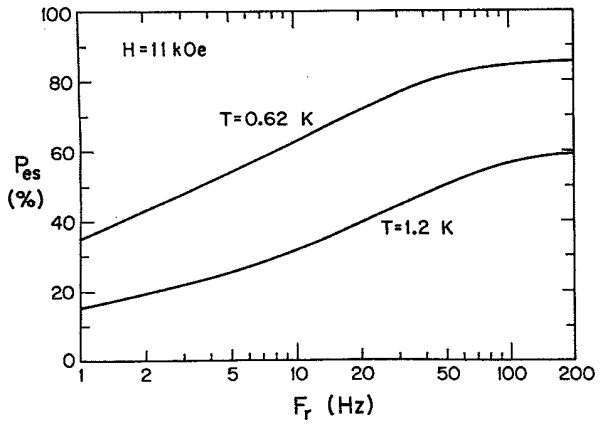

FIG. 2. Calculations of the steady state Yb ion polarization at crossover as a function of rotation frequency for $H = 11$ kOe at temperatures of 0.62 K and 1.2 K.

Langley and Jeffries,[5] is given by

$$T_{1n}^{-1} = 1.8 \times 10^{-14} c H^3 \sin^2\theta \cos^3\theta / \sinh\chi \cosh\chi \ \sec^{-1} , \tag{5}$$

where c is the ratio of Yb to Y atoms in percent. Experimentally one finds that the angular dependence of T_{1n}^{-1} is in good agreement with this formula.[5,8] The numerical constant in Eq. (5) has been chosen to optimize the fit to the data of Ref. 5.

III. EXPERIMENTAL DETAILS

The experiments were carried out in the liquid-helium dewar shown schematically in Fig. 3. The sample is cooled by pumped liquid ^{3}He. The ^{3}He gas, which circulates in a closed loop, enters the dewar through a heat exchanger cooled by ^{4}He vapor. The ^{3}He line then passes through the liquid ^{4}He and into a pumped ^{4}He reservoir where the ^{3}He liquifies. The ^{3}He then expands through a needle valve, which can be adjusted from outside the dewar, and the resulting spray is directed at the YES sample. The evaporating ^{3}He gas is pumped away by a 140 l/sec roots pump backed by a 17 l/sec mechanical pump. Before reentering the dewar the ^{3}He is passed through an oil filter and a liquid nitrogen cooled molecular sieve trap. The cooling system can maintain a temperature of 0.6 K with a heat load of 60 mW.

The temperature in the sample region is monitored with an accurately calibrated germanium resistor located about 2.5 cm from the sample. The temperature gradients near the sample are not expected to be large since the sample is quite far from major sources of heat (i.e., the bearings) and from the pool of liquid ^{3}He at the bottom of the sample tube. Consequently the sensing resistor should give a reliable indication of the ^{3}He vapor temperature at the surface of the sample.

The YES crystals are held in Kel-F containers which are attached to a shaft capable of rotating at rates of up to 100 revolutions per second. The low-temperature end of the shaft is made of an epoxy-Fiberglass material

(*G*-10) and is 2.5 cm in diameter. The upper end of the shaft is coupled to a motor located outside the vacuum system through a Ferrofluidic[15] feedthrough. The shaft is supported by commercial high precision stainless steel ball bearings which have been modified in two respects. First, the balls and races were thoroughly cleaned and then plated with a thin coating of tungsten disulfide,[16] which is an effective solid lubricant. Second, the commercial stainless-steel ball separators were replaced with specially machined separators made of Duroid,[17] a Fiberglass-filled Teflon material. We have found these modified bearings to be very reliable, whereas unmodified bearings often failed after only a few hours of operation.

The required magnetic fields are provided by two internal superconducting magnets. Since the rotation axis of the crystals is vertical, the field used for polarizing must

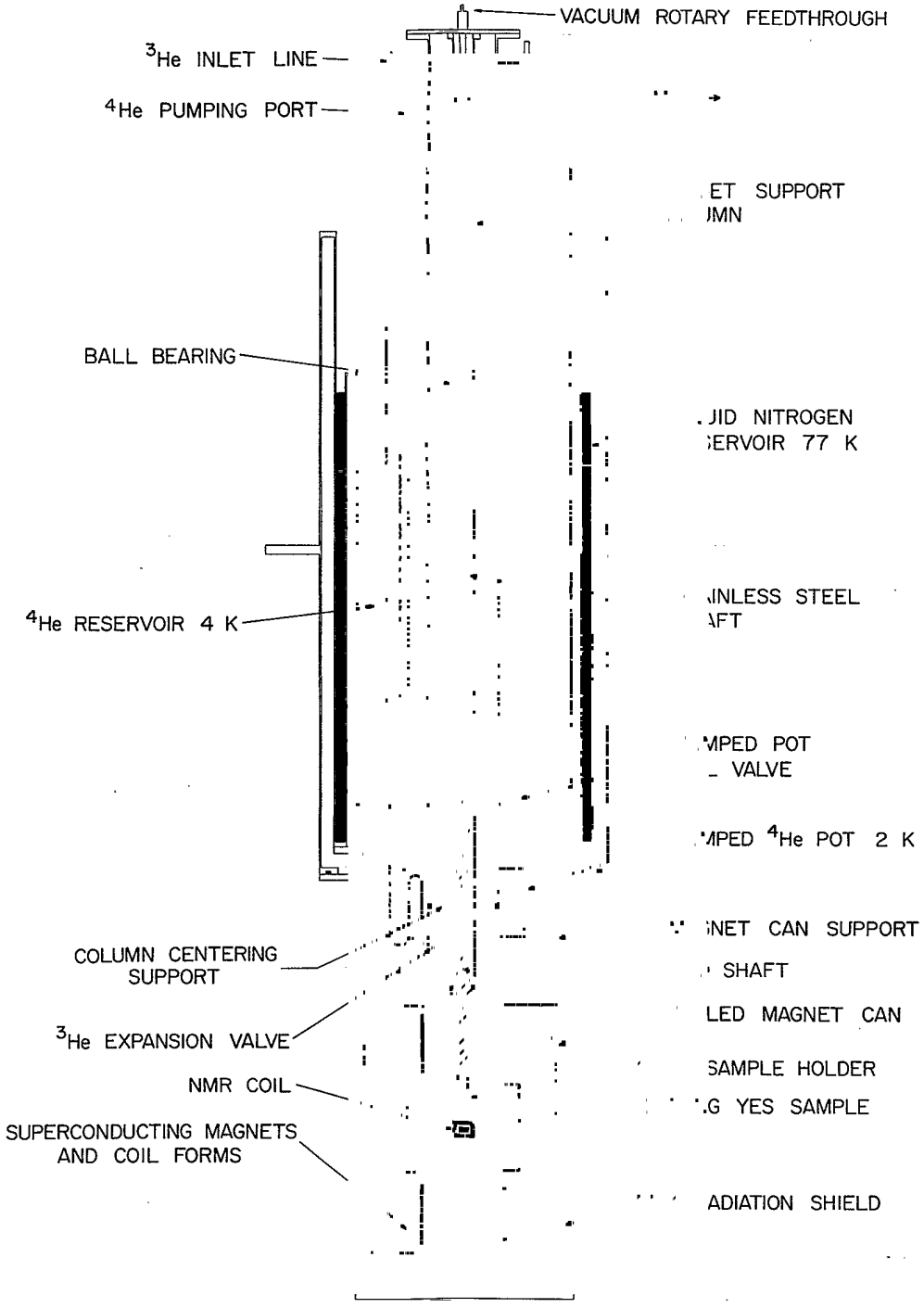

FIG. 3. Schematic diagram of the experimental apparatus.

be horizontal. Two saddle-shaped coils are used to produce a field of up to 11 kOe for this purpose. The second superconducting magnet consists of four circular coils in a split pair configuration designed to produce a vertical magnetic field uniform to $\pm 0.5\%$ over a cylindrical volume 6 cm in diameter and 8 cm high. For the experiments described in the present paper this magnet was used primarily for NMR measurements of the sample polarization; however, the magnet design is such that it can also be used to provide a uniform holding field for the larger targets which we will use in subsequent nuclear physics experiments.

The method used to measure the polarization of the sample is similar to that described by Potter.[18] A block diagram of the NMR electronics is shown in Fig. 4. The tank circuit consists of an LC circuit in which the inductor consists of a few loops of wire surrounding the YES sample. The capacitors are chosen so that the circuit resonates at $f=10$ MHz. The magic tee splits the crystal stabilized radio frequency signal and sends it to the tank circuit and a similar balancing circuit. The reflected signals from the two circuits are then added together 180° out of phase. The resulting output from the magic tee is then amplified, rectified and amplified again. By carefully adjusting cable lengths and capacitors in the balance circuit it is possible to tune the circuit so that the output from the magic tee is sensitive only to the absorptive part of the NMR response. To detect the NMR absorption the magnetic field is swept back and forth through the resonance line at a frequency of about 1.4 Hz. The sweep width is about 56 Oe (peak to peak) which corresponds to about twice the observed full width at base of the absorption line. The magnetic field is adjusted so that the resonance line appears at the center of the sweep. A lock-in amplifier is used to pick out the absorption signal which occurs at a frequency of double the sweep frequency.

The absolute normalization of the polarization is determined by measuring the thermal equilibrium signal at $T=4.2$ K. At this temperature the Yb ion spin-relaxation is dominated by the Orbach process[7] and is much more rapid than at our normal operating temperatures. The hyperfine coupling gives rise to a proton spin-relaxation time of about 4 sec, and therefore the polarization can be calculated from the Boltzmann equation.

For our conditions the thermal equilibrium polarization is only about 6×10^{-5}, and since we need to measure polarizations a factor of 10^4 larger, the linearity of the system is important. To achieve linearity, care was taken to insure that the size of the rf signal at the input of the rf detector was such that the rectifier circuit operated in a linear range. With polarizations near 50% the rf level at the detector changes by only about a factor of 2 as the field is swept from off resonance to on resonance. It was also necessary to adjust the resistance of the tank circuit so that the power absorbed by the protons is small compared to the power dissipated in the circuit itself (so the Q of the circuit does not change significantly). We estimate that systematic errors in the measurement of the polarization are less than 10% of the measured value.

A variety of techniques were used to prepare the YES solutions and grow the crystals. In the end, a method similar to that described by Felcher *et al.*[13] was adopted. In most cases, the Yb used was 99% isotopically enriched ^{174}Yb. The Yb/Y ratios in the crystals ranged from 0.005 to 0.048 %, as determined either by proton-induced x-ray emission (PIXE) or by neutron activation analysis.

We performed measurements on two types of samples. The first, which we call granular, consisted of a large number of small single crystals with irregular dimensions of about 1–2 mm. These were randomly oriented and held in a Kel-F cylinder with a diameter and height of 1 cm. The second type of sample was a $1\times 0.7\times 0.5$ cm single crystal. In this case the crystal c axis was aligned at an angle 80° from the vertical. This orientation is chosen so that the protons do not couple strongly to the Yb ions when the vertical field magnet is in use. As we spin the target to polarize the protons, the angle between the polarizing field (which is horizontal) and the c axis of

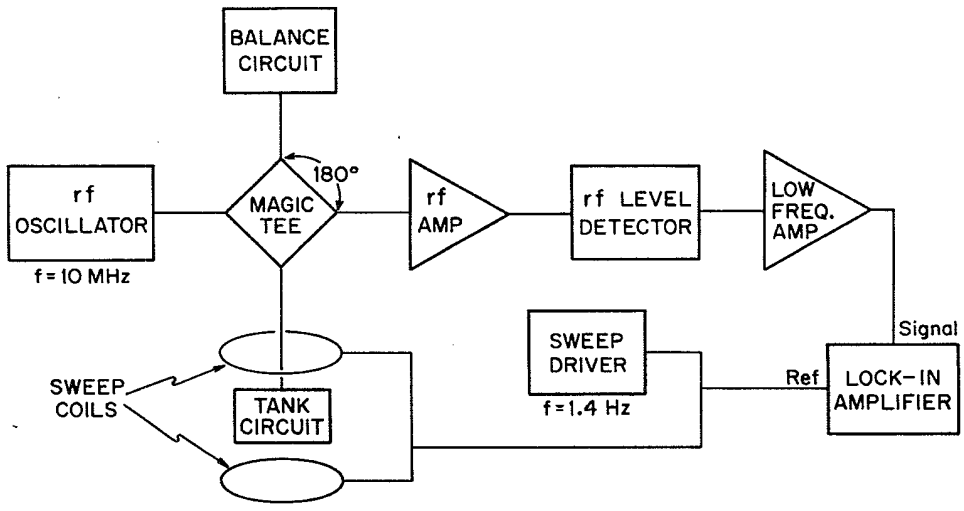

FIG. 4. Schematic diagram of the NMR electronics used to measure the proton polarization.

TABLE I. Properties of the YES samples used in the present experiment. In the second column, g is used to designate granular samples and s single crystals. The third column gives the Yb concentration of the crystals.

Sample	Type	Yb concentration (%)
1	g	0.005[a]
2	g	0.014[a]
3	g	0.021
4	g	0.037
5[b]	g	0.010
6	g	0.025
7	s	0.048
8[b]	s	0.010
9	s	0.008
10[c]	s	0.005
11[c]	s	0.006
12[c]	s	0.009
13[c]	s	0.009[a]

[a]Inferred from Yb concentration of growing solution.
[b]Obtained from Hinks, Argonne National Laboratory.
[c]Relaxation-time measurements only.

the single crystal varies between 10° and 170°, and passes through 90° twice per revolution. As noted above, the 90° orientation is essential since this is where the level crossings occur. Since the cycle involves angles with $\cos\theta \sim 1$, the Yb g factor is large during an appreciable portion of the cycle, and therefore one obtains sizable Yb polarizations.

The properties of the various samples used are listed in Table I. Here g is used to denote granular samples and s single crystals. Note that for samples 10–13 we only report measurements of the proton spin-relaxation times. These last few samples have been used in a more recent set of experiments with a working polarized target which differs in several respects from the apparatus described above. In view of the extensive modifications, it did not seem appropriate to incorporate the proton polarization results into the present paper. On the other hand, the relaxation times should not be affected by the modifications, and therefore these data have been included.

IV. EXPERIMENTAL RESULTS

A. Maximum polarizations

In Table II we present a complete list of measurements of the maximum proton polarization achieved under a wide range of conditions. The results are listed in chronological order and cover a time span of about one and a half years. One notes, first of all, that there is a gradual increase in the observed maximum polarization as a function of time. We believe that these improvements resulted from a combination of many factors, including the use of higher magnetic fields and higher rotation rates, improvements in the cooling system and in various mechanical components of the target, the change from granular samples to single crystals and the use of samples with lower Yb concentrations.

The maximum polarizations obtained with granular samples are clearly lower than those observed with single crystals. For example, with sample 5 (a granular sample) we obtain $P_n = 32\%$ at $F_r = 41$ Hz, $H = 11$ kOe whereas with sample 8 (a single crystal grown at the same time) we obtain $P_n = 48\%$ under essentially the same conditions. Although some loss in polarization is expected for a granular sample due to the random orientation of the crystals, this effect should only reduce the Yb ion polarization at crossover by about 8% (Ref. 19), which is not sufficient to explain the observed differences. We believe that the main problem has to do with the internal heating of the crystals which results from coupling of the Yb spins to the lattice (see Ref. 10). Since ^{3}He vapor is a very poor thermal conductor, heat generated near the center of the granular sample is not dissipated effectively. Adding liquid to the sample holder is also thought to be ineffective, since the heat generated produces large volumes of the ^{3}He vapor which prevent liquid from ever reaching the center of the sample. A single crystal can be cooled more effectively, since the thermal conductivity of YES is large compared to that of the ^{3}He vapor. This provides a mechanism to transport the heat to the surface of the sample where it can be removed by the ^{3}He spray from the expansion valve. With single crystal samples we were able to obtain polarizations in excess of 50%.

In spite of the improvements, the observed polarizations for single crystals are still well below the calculated Yb ion polarization at crossover. As noted in Sec. II A, the polarization of the protons is expected to reach that of the Yb ions provided that the polarization is transferred through a process in which one Yb ion flips spin with a single proton. The failure of this simple picture to explain the observed polarizations provided the motivation to develop the model described in Sec. V.

B. Polarization buildup curves

Polarization buildup curves were measured by interrupting the spinning for short periods of time to measure the polarization. The interruptions were short compared to the relaxation time of the proton polarization and hence should have a negligible effect on the shape of the curve. In Fig. 5 the measured polarization is plotted as a function of accumulated spinning time for two representative cases. The calculations shown in Fig. 5 will be discussed in Sec. V.

C. Holding times

In this section we discuss the measurements of the proton spin-relaxation time, T_{1n}. Relaxation times were measured for all 13 of the samples listed in Table I, and in most cases results were obtained for several values of the magnetic field. The temperatures were normally in the range 0.45–0.60 K.

In Fig. 6 we show the experimental results plotted as a function of magnetic field for a number of different samples. Each set of measurements is labeled by the sample

TABLE II. Maximum proton polarizations obtained with various samples, rotation rates, and magnetic fields.

Sample	F_r (rps)	H (kOe)	T (K)	Measured P_n (%)	Predicted P_n (%)
1	18	7.0	0.62	3	
	20	5.0	0.62	3	
	20	7.0	0.62	3	
	30	8.5	0.62	12	
	35	8.5	0.62	11	
2	30	8.5	0.57	9	
3	22	8.5	0.57	13	
	20	5.0	0.60	9	
	30	8.5	0.57	22	
4	80	11.0	0.70	25	
	50	10.0	0.65	22	
5	42	9.0	0.48	20	
	41	11.0	0.48	32	
	70	11.0	0.53	35	
	20	11.0	0.48	38	
6	40	9.0	0.65	27	
	40	11.0	0.65	28	
	40	7.0	0.65	17	
	30	10.0	0.65	26	
	60	10.0	0.73	27	
	80	10.0	0.73	25	
7	40	9.0	0.64	34	34
	40	7.0	0.62	24	22
	40	11.0	0.62	39	41
	60	11.0	0.92	43	45
8	40	9.0	0.62	33	41
	40	11.0	0.62	48	53
	60	11.0	0.86	52	47
	90	11.0	0.96	53	49
9	40	9.0	0.57	43	43
	40	11.0	0.57	59	56
	85	11.0	0.65	57	66
	100	11.0	0.62	44	71

number and by the temperature at which the measurements were obtained. Although there is a considerable amount of variation from one sample to another, in the best cases we obtain holding times in excess of 100 h for magnetic fields of less than 1000 Oe. The spin-relaxation times are quite long even for very low magnetic fields; for example, at 20 Oe the observed holding time for sample 8 was approximately 3 h. The spin-relaxation times predicted from Eq. (5) are more than an order of magnitude longer than the observed holding times, and therefore we conclude that the relaxation of the proton spins cannot be attributed to the mechanism described in Ref. 5.

The dashed line in Fig. 6 indicates the slope that one would expect to obtain under the assumption that $T_{1n} \propto H$. Although there are a few anomalous points, it is apparent that the observed relaxation times are directly proportional to the magnetic field strength. In contrast to the observed behavior, Eq. (5) predicts $T_{1n} \propto H^{-2}$ in the limit of small χ.

Although we have made no systematic study of the temperature dependence of the spin-relaxation rate, the measurements which are available suggest that T_{1n} varies approximately as T^{-2}.

While it is apparent that Eq. (5) does not properly account for the observed spin-relaxation results, it is not clear whether the Yb ions play a role in the depolarization process. To address this question one can look at the dependence of the spin-relaxation rate on Yb concentration. In Fig. 7, measurements of T_{1n} at $H=500$ Oe are plotted as a function of the Yb concentration, c. For several of the samples, the plotted points were obtained by extrapolating measurements obtained at higher magnetic fields, assuming $T_{1n} \propto H$. In addition, the measurements have been extrapolated in temperature, assuming $T_{1n} \propto T^{-2}$, to a common temperature of 0.5 K. For cases in which it was necessary to extrapolate by more than 50 Oe or by more than 0.05 K the results are shown as open circles.

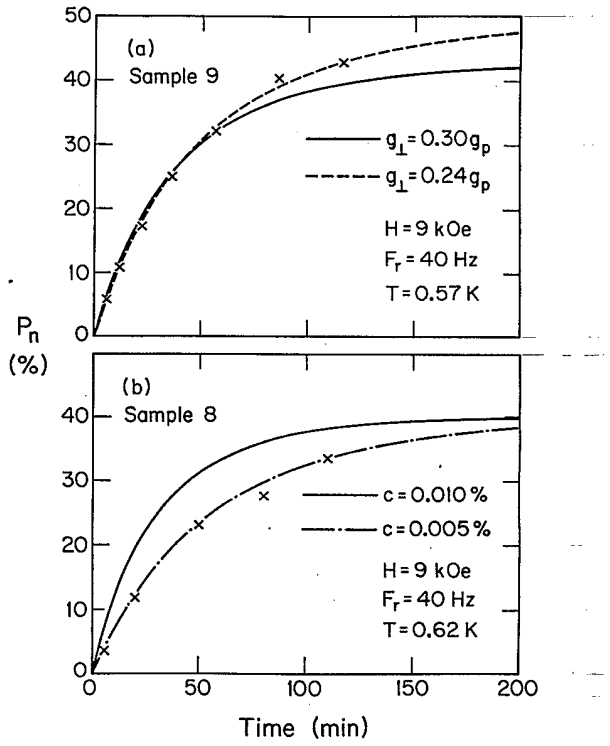

FIG. 5. Measurements of the proton polarization as a function of accumulated spinning time for two YES single crystal samples. The curves are predictions obtained from model calculations described in Sec. V. In each case the solid curve corresponds to our standard parameter set.

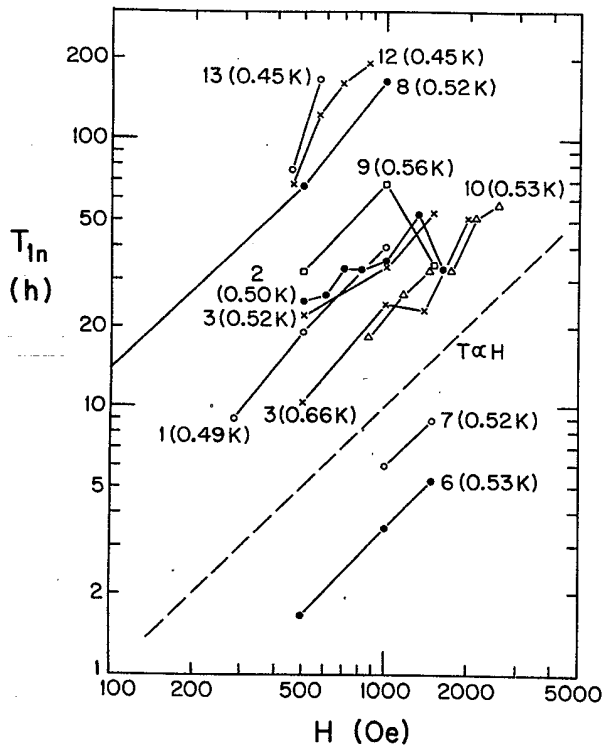

FIG. 6. Measurements of the proton spin-relaxation time for various samples plotted as a function of magnetic field. Each set of measurements is labeled by the sample number and temperature. There is one additional measurement (not shown) for sample 8 at $H=20$ Oe for which $T_{1n} \simeq 3$ h. The dashed line indicates the expected slope for $T_{1n} \propto H$.

From Fig. 7 it would appear that there is some relationship between the spin-relaxation rate and the Yb concentration. Although there is a large amount of scatter in the points, the dashed curve, corresponding to $T_{1n} \propto c^{-2}$, seems to reproduce the overall trend of the data, which might lead one to conclude that the depolarization is caused by a mechanism that involves two Yb spins. However, this hypothesis appears to be ruled out by previous holding time measurements for crystals with high Yb concentrations. From the results shown in Fig. 7 one would predict that for $c=0.5\%$ the holding time should be roughly 0.02 h for $T=0.5$ K assuming $T_{1n} \propto c^{-2}$. However, Langley and Jeffries[5] observe holding times that are larger than this at a much higher temperature of 1.4 K (see Fig. 11 of Ref. 5) for $c=0.5\%$. (The 2% Yb concentration listed in Ref. 5 refers to the growing solutions. Our experience suggests that the Yb concentrations in the crystals are lower by roughly a factor of 4.)

Another possibility is that the presence of the Yb in the growing solution may have adverse effects on the crystal formation (for example, giving rise to lattice defects) which lead to increased spin-relaxation rates. This is supported by the observation (see Ref. 13) that it is extremely difficult to grow well formed crystals from solutions with high Yb concentrations.

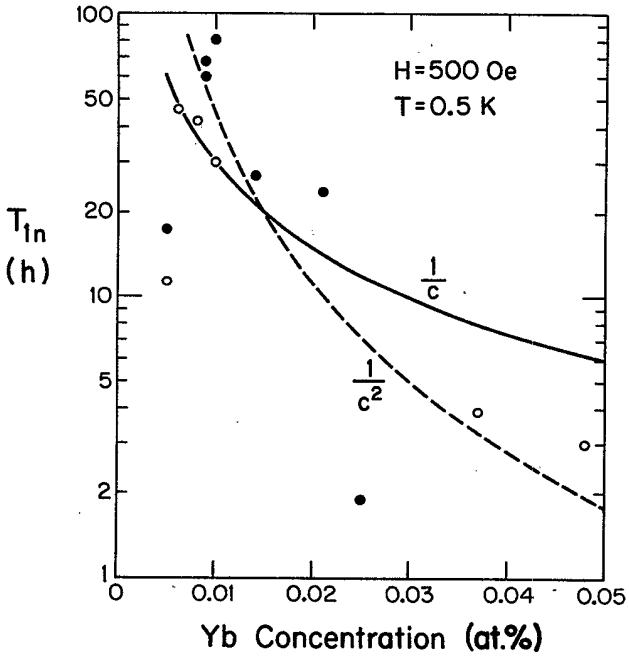

FIG. 7. Measurements of the proton spin-relaxation time for $H=500$ Oe and $T=0.5$ K plotted as a function of the Yb concentration. In many cases the plotted point was obtained by extrapolating measurements obtained at other temperatures and/or fields. Measurements which were extrapolated by more than 50 Oe or more than 0.05 K are shown as open circles.

V. MODEL CALCULATIONS

In order to understand why the measured polarizations are smaller than the calculated Yb ion polarizations at crossover, we have developed a computer-based model of the spin-refrigerator process. Previous authors have, in general, fully described the theory of spin refrigerators, but the calculations presented by these authors have either not included the full range of effects or have been based on simplifying assumptions (e.g., small polarization) which lead to closed form expressions. On the other hand, a computer-based model makes it possible to fully incorporate the important aspects of the existing theory in a realistic way, thereby allowing quantitative comparisons with data. In this section we describe the effects which are included in the model, discuss briefly how the actual calculations are performed, and show some of the model's predictions.

A. Description of the model

There are the three main processes which we have incorporated into the model calculation. The first involves the interaction of the Yb spins with the lattice during the cycle. The second is the cross relaxation process by which the ion polarization is transferred to the protons. The third process is the internal heating of the YES crystals. We will now discuss each of these in order.

The Yb ion polarization, P_e, is followed through the cycle by assuming that at any instant it decays towards the thermal equilibrium value, P_{e0}, with an exponential time constant T_{1e}^{-1} given in Eq. (3); i.e.,

$$\frac{dP_e}{dt}=T_{1e}^{-1}(P_{e0}-P_e) . \tag{6}$$

The thermal equilibrium polarization is a function of the angle θ and is given by

$$P_{e0}=\tanh[g(\theta)\mu_B H/2kT] . \tag{7}$$

If the ion polarization at the start of a given cycle (i.e., immediately following the cross relaxation) is P_{ei}, the polarization at the end of the spin-lattice relaxation portion of the cycle (i.e., just prior to the next cross relaxation) will be[5,7]

$$P_{ef}=K_e P_{es}+(1-K_e)P_{ei} , \tag{8}$$

where

$$K_e=1-\exp\left[-\int_0^{\tau}T_{1e}^{-1}(t)dt\right] \tag{9}$$

and

$$P_{es}=\frac{1-K_e}{K_e}\int_0^{\tau}P_{e0}(t)T_{1e}^{-1}(t) \times\exp\left[\int_0^{t}T_{1e}^{-1}(t')dt'\right]dt . \tag{10}$$

In these formulas, T_{1e}^{-1} and P_{e0} are expressed as functions of time, and τ is the time required to complete one cycle (i.e., $\tau=\frac{1}{2}F_r$). The quantity K_e can be thought of as the spin-relaxation probability per cycle, and P_{es} as the steady-state ion polarization at crossover (i.e., steady state in the sense that if P_e is not altered as the sample passes through the cross relaxation region, the ion polarization will approach this value). It follows that P_{es} is the maximum polarization the protons will acquire for the special case in which only 1:1 spin flips occur. It is this quantity which has been plotted in Fig. 2. It should be noted that the quantities which enter into this part of the calculation $[g(\theta),T_{1e}^{-1}(\theta)]$ are well known.

The second part of the model involves a description of the transfer of polarization from the Yb ions to the protons. The simplest cross relaxation process occurs at some angle near $\theta=90°$, where the mutual spin flip of an Yb ion and one proton is energetically allowed. It is clear that for some angle slightly farther from 90° (i.e., for a slightly larger splitting) it is energetically possible for one Yb ion to flip the spins of two protons (a 2:1 spin flip). At yet another angle, 3:1 processes are energetically allowed, and so on. These multiple–spin-flip processes lead to a reduction in the maximum attainable proton polarization. If only a single ε:1 process takes place the maximum proton polarization will be

$$P_n=\tanh\left[\frac{1}{\varepsilon}\tanh^{-1}P_{es}\right] . \tag{11}$$

This reduction in polarization can be thought of as resulting from the fact that the ions have a higher spin temperature when the multiple spin flips occur than when single spin flips take place.

One can also understand this effect by thinking about the details of the spin-flip process. For example, in the 2:1 process a spin-up ion must interact with two spin-down protons in order for the spin flip to occur. If most of the protons (say for example 90%) already have spin-up, then the spin flip can occur for only a very small fraction of all possible proton pairs (1%). On the other hand, for most of the pairs (81%) both protons have spin-up and can therefore be depolarized by an ion with spin-down. From this numerical example one can see that to achieve a proton spin-up to spin-down ratio of R, one needs the ion spin-up to spin-down ratio to be R^{ε}.

In order to include the multiple–spin-flip processes in the model calculation, it is necessary to know the probability f_ε that the ε:1 spin flip occurs during the cross relaxation part of the cycle. The transition probabilities f_1, f_2, and f_3 were first calculated by McColl and Jeffries.[7] More recently Parker[20] has repeated the calculations for $\varepsilon=1$ and 2 using more recent measurements of the proton positions.[21] The transition probabilities have the general form

$$f_\varepsilon=1-\exp\left[\frac{-b_\varepsilon}{(\omega/2\pi)H^{2\varepsilon-1}}\right] , \tag{12}$$

where ω is defined as $d\theta/dt$ at the cross relaxation point (in radians/sec), H is the magnetic field in Oe, and b_ε is a constant. Note that for the special case in which the crystal c axis and the applied field are both at right angles to the rotation axis, $\omega/2\pi$ is just the rotation frequency,

F_r. If the c axis makes an angle α with the rotation axis ($\alpha=80°$ for our single crystal measurements) then $\omega/2\pi=F_r\sin\alpha$. For $\varepsilon=1$ and 2 we adopt the results obtained by Parker,

$$b_1=8.62\times10^7(g_\perp/g_p)^2[1-(g_\perp/g_p)^2]^{-1/2}\ , \tag{13}$$

$$b_2=2.81\times10^{14}(g_\perp/g_p)^2[1-(g_\perp/2g_p)^2]^{1/2}\ . \tag{14}$$

These results have the same mathematical form as the formulas obtained by McColl and Jeffries, but the numerical constants are larger by a factor of about 2^ε. For b_3 we use the result of McColl and Jeffries, namely

$$b_3=6.15\times10^{19}(g_\perp/g_p)^2[1-(g_\perp/3g_p)^2]^{3/2}\ , \tag{15}$$

but scale it up by a factor of 8 for our calculations. Unless noted otherwise, we use $g_\perp/g_p=0.3$, as suggested in Ref. 10.

In our model calculations we include only $\varepsilon=1$, 2, and 3. This is probably reasonable, since f_3 is already quite small compared to f_1 and f_2 for most of the situations encountered in our experiment. For example, with $H=9$ kOe and $F_r=40$ Hz we obtain $f_1=1$, $f_2=0.58$, and $f_3=0.018$.

Whereas the interaction of the Yb ions with the lattice is well understood, the situation is less clear for the cross relaxation process. First, the calculation of the numerical factors is very sensitive to the Yb-proton separations. Although the geometry of the YES crystal lattice is fairly well known, the uncertainty in the b_ε parameters is probably still appreciable. In addition, the cross relaxation probabilities depend on the parameter $g_\perp$ which, as noted earlier, has never been measured directly.

The final ingredient in the model is the internal heating. The heating has been discussed extensively by Potter and Stapleton,[10] and is caused by the fact that the Yb ion polarization always lags behind the thermal equilibrium value, which leads to absorption of energy from the mechanical rotation. The average power dissipated to the lattice, $\langle\dot{q}\rangle$, can be expressed as

$$\langle\dot{q}\rangle=(N_e\mu_B H/2\tau)\int_0^\tau(dp_e/dt)g(t)dt\ , \tag{16}$$

where N_e is the number of Yb ions in the sample. If the ion polarization is known throughout the cycle the heat generated in the crystal is easily calculated. To convert this into a temperature rise we need to determine how rapidly the heat is dissipated by the ^{3}He in our cooling system.

The heat transfer coefficient, defined as $k=\dot{q}/A\Delta T$, where $\dot{q}$ is the dissipated power, A is the surface area of the sample, and ΔT is the temperature difference, was determined experimentally. This was done by placing a brass block, similar in shape and size to our YES single crystals, in the ^{3}He refrigerator. Brass was chosen since its thermal conductivity is close to that of YES.[22] The block contained a temperature measuring resistor and a second resistor used as a heater. By measuring the temperature rise for various power settings in the sample, the heat transfer coefficient was determined to be about 0.2 mW/K cm^2.

B. Details of the computer calculations

In order to determine the maximum attainable proton polarization and also to make predictions for the polarization buildup curves, we have developed a computer program which incorporates the processes described in Sec. V A. In the computer calculations we make use of the fact that the protons greatly outnumber the Yb ions (typically by a factor of 10^5 or more) in our YES samples. It follows that the proton polarization changes very little over the course of a few cycles. On the other hand, the Yb polarization is continually changing as the ions interact with the lattice and as the crystal rotates through the cross-relaxation region. The first step in the computer calculation is to determine how the Yb polarization varies over any given spin-refrigerator cycle.

Suppose that at some instant the protons have a polarization P_n. In order to determine how the Yb polarization behaves for this value of P_n we begin by postulating some value, P_{ei}, for the polarization of the ions at the start of the cycle (i.e., immediately following the cross relaxation). We then begin to follow the Yb polarization through the spin-refrigerator cycle. In the first step the ions relax to the lattice and the polarization changes to a new value, P_{ef}, given by Eq. (8). The second part of the cycle consists of a series of six proton-Yb cross relaxations, in the order 3:1, 2:1, 1:1, 1:1, 2:1, 3:1. If the Yb polarization prior to a given ε:1 cross relaxation is P_{ei}, the polarization after the cross relaxation will be

$$P_{ef}=f_\varepsilon P_{e\varepsilon}+(1-f_\varepsilon)P_{ei}\ , \tag{17}$$

where $P_{e\varepsilon}$ is the polarization which would result if the cross relaxation were complete; i.e.,

$$P_{e\varepsilon}=\tanh(\varepsilon\tanh^{-1}P_n)\ . \tag{18}$$

In the computer calculation one simply follows the Yb polarization for a number of spin-refrigerator cycles (assuming constant polarization) until the Yb polarization has reached an equilibrium state in which the value of P_ε at the end of a given cycle is the same as at the corresponding point in the previous cycle. Normally this convergence takes place within two or three cycles.

At this point heating effects are included. Having determined the appropriate starting value for P_e, $P_e(t)$ is determined throughout the spin-lattice relaxation portion of the cycle by numerical integration of Eq. (6), and the heat generated is then calculated from Eq. (16). The internal temperature of the crystal is obtained from $\langle\dot{q}\rangle$, the assumed ambient temperature and the measured heat transfer coefficient. We then go back to the beginning and redetermine the Yb polarization throughout the cycle using the corrected crystal temperature (in the initial calculation the crystal temperature is assumed to be equal to the ambient temperature). The entire process of calculating $\langle\dot{q}\rangle$ and redetermining $P_e(t)$ is then repeated as necessary until the values obtained for $\langle\dot{q}\rangle$ converge (normally three or four iterations are sufficient).

Having now obtained what should be the correct Yb polarization throughout the cycle it is a simple matter to determine the change in the nuclear polarization. For a

given ε:1 cross relaxation the change in the nuclear polarization is given by

$$\Delta P_n = -\varepsilon r \, \Delta P_e \ , \tag{19}$$

where ΔP_e is the change in the Yb polarization and r is the ratio of the number of Yb ions to the number of protons in the sample. The computer calculations thus permit us to determine ΔP_n for a complete cycle for any assumed value of P_n. This makes it possible to map out the polarization buildup curve and to find the maximum attainable polarization.

C. Model predictions

In Fig. 8 we plot the model predictions of the maximum proton polarization as a function of rotation rate for $H=7$, 9, and 11 kOe at 0.62 K. The dot-dash curves are included for reference and show the expected proton polarization for the case in which multiple spin flips and internal heating are neglected. For this calculation the predicted proton polarizations are large even for relatively low magnetic fields and rotation rates (e.g., 7 kOe and 10 Hz). The inclusion of multiple spin flips (solid lines) greatly reduces the expected polarization, particularly at lower rotation rates and fields. For high rotation rates ($F_r > 30$ Hz) P_n is predicted to depend very strongly on magnetic field. This results from the fact that higher fields lead to a substantial reduction in the multiple spin flip probabilities, f_2 and f_3.

The multiple–spin-flip processes lead to a larger reduction in P_n than one might have expected on the basis of naive considerations, as the following example will illustrate. At $H=9$ kOe, $F_r=40$ Hz (where f_1 and f_2 are both large and f_3 is essentially negligible) the steady state Yb polarization is found to be 77%. It follows that for a pure 1:1 process one would obtain $P_n=77\%$, whereas the expected polarization for a pure 2:1 process is, according to Eq. (11), $P_n=47\%$. However, the predicted model polarization is only 42% (see Fig. 8). In fact, it is quite generally true that when f_1 and f_2 are both large, the 1:1 and 2:1 process working together produce a polarization that is lower than that for either process by itself.

The explanation for this rather unexpected result can be found by considering the details of the cross-relaxation process. For simplicity let us assume that in the steady state, the Yb polarization at crossover is 100%. It follows that a pure 1:1 process and a pure 2:1 process would both lead to 100% proton polarization. However, if $f_1=f_2=1$ the maximum attainable polarization is only about 56%. To see this let us consider in detail what happens during the cross relaxation phase of the cycle once the nuclear polarization has reached 56%. The cross relaxation begins with the 2:1 process in which P_e is reduced from 100% to 85.3% [see Eq. (18)], thereby increasing P_n by $2(0.147)r$. This is followed by a sequence of two 1:1 processes. Here P_e drops to 56% and consequently P_n increases by an additional $1(0.293)r$. However, in the final step the nuclear polarization is reduced. This last step is another 2:1 relaxation, which means that P_e returns to 85% thereby reducing P_n by $2(0.293)r$. As one can see, the net change in the nuclear polarization is zero. It is this interplay between the 1:1 and 2:1 process that gives rise to the large polarization losses which are evident in Fig. 8.

We now turn to the internal heating mechanism. The effects of internal heating are found to be small but not negligible. The dashed curves in Fig. 8 show the predicted polarizations for $k=0.2$ mW/K cm^2 (appropriate for our measurements with single crystals) and $c=0.02\%$. It appears that internal heating effects are important only under conditions for which the expected nuclear polarization is large. For cooling systems in which there is better thermal contact between the crystal and the coolant the effects of internal heating will be smaller.

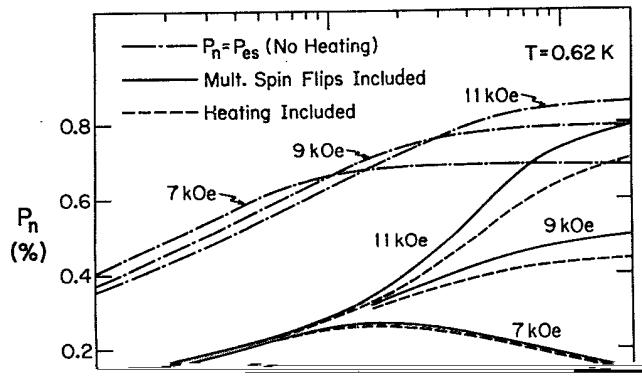

VI. COMPARISON OF THEORY AND EXPERIMENT

A. Maximum polarization

In Table II our measurements of the maximum proton polarization are compared with model calculations including multiple spin flips and internal heating. Since we do not have a quantitative understanding of how the internally generated heat is dissipated in the granular samples, the model predictions are given only for the sin-

least, these results demonstrate clearly (for the first time) the importance of multiple spin flips in the cross relaxation process. Moreover we conclude that the $g_\perp$ and b_ε values used in the calculations must be at least approximately correct.

In Table III we compare the model predictions with the rotating crystal measurements of Felcher *et al.*[13] Once again we find reasonably good agreement between the measurements and calculations. In this case the measurements are always smaller than the calculations, but this is to be expected since the internal heating was neglected in these calculations (since the heat transfer coefficient is not known). Note that the agreement is best for low rotation rates and fields where the heating is least.

Felcher *et al.*[13] have also reported measurements for a rotating or pulsed magnetic field rather than a rotating crystal. Table IV shows the model calculations for this situation. The agreement is again quite reasonable, particularly in view of the fact that the calculated 3:1 spin-flip probability is quite large for many of these cases (see Table IV), which raises the possibility that higher-order processes, not included in the model, may be non-negligible. In any case, it is clear that the measurements in Table IV cannot be reproduced if one neglects multiple spin flips.

The largest polarizations ever reported for YES are those of Button-Shafer *et al.*[11,12] Under conditions similar to those of Felcher *et al.*[13] these authors have reportedly achieved polarizations of 65–80 % in granular samples rotated at $F_r \simeq 100$ Hz. Under the stated experimental conditions ($T=1.25$ K, $H=10.7$ kOe) our model predicts that for a randomly oriented granular sample with no internal heating, the maximum proton polarization should be 32%, which is far less than the reported values. In fact the steady state Yb ion polarization at crossover, P_{es}, for crystals oriented at the optimum angle is only 54%. Since the reported polarizations exceed this straightforward and absolute upper limit by a substantial amount, we are convinced that the measurements are incorrect.

TABLE III. Comparison of proton polarization data from Ref. 13 to the model.

F_r (sec^{-1})	H (kOe)	T (K)	Measured P_n (%)	Predicted P_n (%)
50–150	0.0	1.22	0	0
50	7.65	1.22	16	18
50	10.0	1.21	25	28
50	12.5	1.21	29	33
50	14.7	1.21	32	36
100	7.65	1.21	17	18
100	10.0	1.21	25	36
100	12.5	1.21	34	47
100	14.6	1.21	37	49
150	7.75	1.21	13	17
150	10.0	1.21	28	39
150	12.5	1.21	36	53
150	14.6	1.21	41	56
150	14.6	1.29	36	53
150	0.0	1.21	0	0
150	12.9	1.21	36	54
150	13.2	1.14	41	58

TABLE IV. Comparison of rotating field data from Ref. 13 to the model. The probability of 3:1 spin flips, f_3, is shown in the last column.

H_{DC} (kOe)	H_{AC} (kOe)	Measured P_n (%)	Predicted P_n (%)	f_3
2.85	4.60	3	5	0.91
2.85	6.30	7	9	0.83
2.87	8.50	14	15	0.71
3.02	4.65	3	6	0.85
3.02	6.30	7	10	0.76
3.02	8.50	13	16	0.6
3.48	6.30	10	11	0.54
4.00	6.30	11	13	0.36
5.00	6.30	12	16	0.17
6.00	6.30	18	17	0.08

B. Polarization buildup curves

In Fig. 5 measurements of polarization buildup curves are compared with predictions of the model. The results in Fig. 5(a) are for sample 9 at $H=9$ kOe, $F_r=40$ Hz, and $T=0.57$ K, while those in Fig. 5(b) are for sample 8 at $H=9$ kOe, $F_r=40$ Hz, and $T=0.62$ K. In both cases the solid curve represents our "standard" model calculation with $g_\perp=0.3g_p$ and with the Yb concentration taken to be the measured value from neutron activation.

In the first example we find that the standard calculation does a good job of reproducing the initial buildup rate, but that the last two data points are somewhat higher than the predicted curve. The dashed curve, obtained by changing the assumed value of $g_\perp$ to $0.24g_p$, does a much better job of reproducing the measurements. This change reduces the probability for multiple spin flips and consequently increases the ultimate polarization without substantially altering the initial buildup rate. We do not consider it surprising that small changes in the value of $g_\perp$ are beneficial. In fact it is probably an oversimplification to suppose that $g_\perp$ has a single unique value. Since nonzero values of $g_\perp$ can arise at least in part from crystal defects, it is possible that the average value of $g_\perp$ for any given crystal depends on such things as the Yb concentration[9] and other details of the crystal growing procedure. Furthermore, it may well be that the Yb ions within a given crystal have a distribution of $g_\perp$ values, ranging from essentially zero to several times the average value.

For the case shown in Fig. 5(b) the standard calculation fails to reproduce the initial polarization buildup rate. However, one can reproduce the observations by reducing the assumed Yb concentration by about a factor of 2. As shown by the dot-dashed curve, this decreases the initial buildup rate without affecting the ultimate po-

larization very much. This same kind of effect has been observed for all of the crystals which were grown by the method described in Ref. 13, in which the growing solution contains excess Ba. This suggests that some fraction of the Yb ions in these crystals may be located at positions other than the standard Y lattice site. If this is the case, these Yb ions will not have a highly anisotropic g factor, and consequently will not participate in the spin-refrigerator process.

We find that overall the computer model does a good job of reproducing measurements of polarization buildup curves. Although there are often minor discrepancies with the standard model calculations, we find that one can always obtain a good fit with parameters which are at least plausible. This reinforces our conclusion that multiple spin flips play an important role and that the $g_\perp$ and b_ϵ parameters used are at least approximately correct.

VII. SUMMARY AND CONCLUSIONS

We have obtained new experimental results on the spin-refrigerator method for polarizing protons in yttrbium-doped ytterium ethyl sulfate at temperatures near 0.6 K. Proton polarizations of greater than 50% have been obtained in single crystals with Yb concentrations of about 0.01% rotated at 40–90 resolutions/sec in fields of 11 kOe.

A computer-based model of the spin-refrigerator process which incorporates effects discussed by previous authors has been developed. Overall, the model does a good job of reproducing measurements of polarization buildup curves and of the maximum polarization. The model calculations show that multiple spin flips play an important role in the Yb-proton cross relaxation process. Furthermore, it is apparent from the success of the model calculations that the parameters which determine the multiple–spin-flip probabilities are reasonably well known. The multiple spin flips lead to a substantial reduction in the maximum attainable proton polarization. This effect is most evident at low-rotation rates and low fields. The computer model does an adequate job of explaining the measurements of Felcher *et al.*,[13] but can not reproduce the high polarizations reported by Button-Shafer *et al.*[11,12] Since these latter measurements also exceed straightforward upper limits on the polarization, we conclude that these measurements must be incorrect.

The main element of uncertainty in the model calculations is the parameter $g_\perp$. A direct measurement of this quantity would be an important step forward in our understanding of the spin-refrigerator process.

Proton spin relaxation times in excess of 100 h have been observed for fields of less than 1 kOe. The relaxation time for any given sample is observed to be directly proportional to H. The measured holding times appear to be correlated with Yb concentration, but it is unclear to what extent the Yb ions are directly responsible for the spin relaxation. The depolarization mechanism described in Ref. 5 is definitely not the dominant process in the present experiment.

The development of YES spin refrigerators has now progressed to a point at which it is feasible to construct working polarized proton targets with polarizations in excess of 50% for experiments in high energy and nuclear physics. The main advantage of spin-refrigerator targets is that long holding times can be achieved in very low magnetic fields.

ACKNOWLEDGMENTS

The authors wish to thank Tom Casavant, Genevieve Orr, Steve Arant, and Lisa Bernstein for their important contributions to various aspects of the experimental work. We are also indebted to Dr. Wendell Potter for a number of enlightening discussions concerning the interpretation of our experimental results, and to Dr. David Hinks for advice on growing YES crystals and for providing some of his crystals. This work was supported in part by the U.S. Department of Energy under Grant No. DE-AC02-79ER10410.

---

*Present address: Indiana University Cyclotron Facility, 2401 Milo B. Sampson Lane, Bloomington, Indiana 47405.

[1]T. J. Schmugge and C. D. Jeffries, Phys. Rev. Lett. **9**, 268 (1962).

[2]C. D. Jeffries, Cryogenics **3**, 41 (1963).

[3]A. Abragam, Cryogenics **3**, 42 (1963).

[4]K. H. Langley and C. D. Jeffries, Phys. Rev. Lett. **13**, 808 (1964).

[5]K. H. Langley and C. D. Jeffries, Phys. Rev. **152**, 358 (1966).

[6]J. R. McColl and C. D. Jeffries, Phys. Rev. Lett. **16**, 316 (1966).

[7]J. R. McColl and C. D. Jeffries, Phys. Rev. B **1**, 2917 (1970).

[8]H. B. Brom and W. J. Huiskamp, Physica **60**, 163 (1971).

[9]H. B. Brom and W. J. Huiskamp, Physica **66**, 43 (1973).

[10]W. H. Potter and H. J. Stapleton, Phys. Rev. B **5**, 1729 (1972).

[11]J. Button-Shafer, R. L. Lichti, and W. H. Potter, Phys. Rev. Lett. **39**, 677 (1977).

[12]J. Button-Shafer, in *High Energy Physics with Polarized Beams and Polarized Targets (Argonne, 1978)*, Proceedings of the Third International Symposium on High Energy Physics With Polarized Beams and Polarized Targets, AIP Conf. Proc. No. 51, edited by G. H. Thomas (AIP, New York, 1979).

[13]G. P. Felcher, R. Kleb, D. G. Hinks, and W. H. Potter, Phys. Rev. B **29**, 4843 (1984).

[14]J. P. Wolfe and C. D. Jeffries, Phys. Rev. B **4**, 731 (1971).

[15]Obtained from Ferrofluidics Corporation, Burlington, Massachusetts 01803.

[16]The bearings were obtained from New Hampshire Ball Bearing, Inc., Peterborough, New Hampshire, and were plated by Rotary Components, Inc., Dicronite Division, Covina, California 91723.

[17]Obtained from Rogers Corporation, Rogers, Connecticut 06263.

[18]W. H. Potter, Rev. Sci. Instrum. **45**, 1288 (1974).

[19]This reduction factor was determined by carrying out model calculations (described in Sec. V) for all possible orientations

of the crystal and taking the appropriate average of the predicted polarization. The exact value of the reduction factor depends to some extent on the choice of operating parameters.

[20]D. S. Parker, Ph.D. thesis, University of Illinois at Urbana-Champaign, 1970.

[21]R. W. Broach, J. M. Williams, G. P. Felcher, and D. G. Hinks, Acta Crystallogr. B **35**, 2317 (1979).

[22]P. V. E. McClintock and H. M. Rosenberg, Pure Appl. Cryogenics **4**, 107 (1965); *Proceedings of the International Institute of Refrigeration,* Commision 1 Grenoble, 1965 (Pergamon, New York, 1965).